Indian Journal of Pure & Applied Physics
Vol. 50, October 2012, pp. 719-726

Molecular structure, vibrational spectra and theoretical NBO, HOMO-LUMO analysis of *N*-benzoyl glycine by DFT and *ab-initio* HF methods

Zhang Rui-Zhou[a,b], Li Xiao-Hong[a,b]* & Zhang Xian-Zhou[c]

[a]College of Physics and Engineering, Henan University of Science and Technology, Luoyang 471003 China

[b]Luoyang Key Laboratory of Photoelectric Functional Materials, Henan University of Science and Technology, Luoyang 471003, China

[c]College of Physics and Information Engineering, Henan Normal University, Xinxiang 453007 China

*E-mail:zrzhou@yeah.net

Received 17 November 2011; revised 19 April 2012; accepted 11 June 2012

The vibrational frequencies of N-benzoyl glycine in the ground state have been calculated using density functional method (B3LYP) by using 6-311++G(d,p) basis set. Theoretical vibrational spectra have been interpreted by means of potential energy distribution (PEDs) using MOLVIB program. The equilibrium geometry and the thermodynamic functions of the title compound have been performed at HF/6-31G(d,p)/6-311++G(d,p) and B3LYP/6-31G(d,p)/ 6-311++G(d,p) levels of theory. A detailed interpretation of the infrared spectra is reported. The theoretical spectrograms for IR and Raman spectra have been constructed. The natural bond orbital analysis has been carried out to explain the charge transfer or delocalization of charge due to the intra-molecular interactions. Energies of the highest occupied molecular orbital (HOMO) and lowest unoccupied molecular orbital (LUMO) have been predicted.

Keywords: *N*-benzoyl glycine, Vibrational spectra, HF *ab-initio* calculation, DFT, NBO analysis

1 Introduction

Organic materials have attracted a lot of attention because of their second-order non-linear optical (NLO) susceptibilities and potential applications in electro-optic modulation[1,2], frequency conversion and THz wave generation[3]. Among organic NLO materials, amino acids show the specific features such as absence of strongly conjugated bonds, molecular chirality and zwitterionic nature of the molecule[4]. Further, amino acids contain a proton donor carboxyl acid group and the proton acceptor amine group and thereby creating "push-pull" type motif to enhance the NLO response. γ-Glycine is an interesting NLO material is a colourless NLO crystal with chemical formula $C_6H_5CONHCH_2COOH$ and belongs to glycine family and *N*-benzoyl glycine (NBG) is also called hippuric acid. Recently, Jayarama *et al*[5]. reported the crystal growth, characterization, structural characteristics of NBG. But so far no theoretical work is done on vibration spectra of NBG because of their high complexity and low symmetry. Therefore, the structure and vibrational frequencies of NBG have been studied.

Density functional theory (DFT) approach, especially B3LYP functional, has been previously shown to provide an excellent compromise between accuracy and computational efficiency of vibrational spectra for large and medium size molecules. In addition, vibrational frequencies obtained by quantum chemical calculations are typically larger than their experimental counterparts. So empirical scaling factors are usually used to study the experimental vibrational frequencies.

By using the DFT (B3LYP) method, we have calculated the geometric parameters and the vibrational spectrum of NBG in the ground state and compared with the experimental vibrational frequencies. Hartree–Fock computations are also performed. Vibrational assignments have been carried out on the basis of potential energy distributions (PED) and experimental data. In addition, natural bonding orbital (NBO) analysis was also carried out in order to have any intramolecular charge transfer (ICT) within the molecule. In addition, the energies of the highest occupied molecular orbital (HOMO) and the lowest unoccupied molecular orbital (LUMO) of NBG in the ground state are calculated by using B3LYP method with 6-311++G(d,p) basis set.

2 Computational Details

Calculations of structural parameters, atomic charges, vibrational frequencies, IR and Raman intensities of NBG (Fig. 1) were carried out using

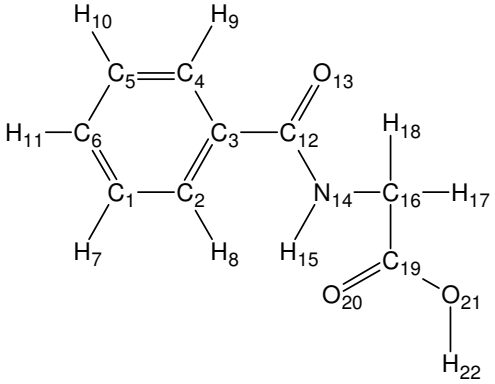

Fig. 1 — Molecular structures and atom numbering scheme of the title compound

Gaussian03 program package[6] by using RHF and DFT approaches.

Initially, the geometry optimization and calculation of other parameters were performed at restricted Hartree–Fock (RHF) level using 6-31G(d,p) basis set. Electron correlations were included using Becke3-Lee-Yang-Parr (B3LYP) procedure[7]. The optimized geometry at RHF/6-31G(d,p) level was taken as the input structure for the density functional calculation at B3LYP/6-31G(d,p) level. Finally, the optimized geometry at the B3LYP/6-31G(d,p) level was used as starting geometry for calculation at the B3LYP/6-311++G(d,p) level. All the computations have been done by adding polarization function *d* and diffuse function on heavy atoms and polarization function *p* and diffuse function on hydrogen atoms, in addition to triple split valence basis set, for better treatment of polar bonds. All the parameters were allowed to relax and all the calculations converged to an optimized geometry which corresponds to a true energy minimum revealed by the lack of imaginary frequencies. Prior to compare the calculated vibrational frequencies with the experimental counterparts the former have been scaled by appropriate scaling factors.

Furthermore, theoretical vibrational spectra of NBG were interpreted by means of PED with the version V7.0-G77 of the MOLVIB program written by Sundius[8]. The calculated Raman activities (S_i) have been converted to relative intensities (I_i) using the following relationship derived from the basis theory of Raman scattering[9] :

$$I_i = \frac{f(v_0 - v_i)^4 S_i}{v_i\left[1 - \exp\left(\frac{-hcv_i}{kT}\right)\right]} \quad \ldots (1)$$

where v_0 is the exciting frequency (in cm^{-1} units), v_i is the vibrational wavenumber of the i^{th} normal mode, *h*, *c* and *k* are universal constants, and *f* is the suitably chosen common scaling factor for all the peak intensities.

3 Results and Discussion

Jayarama *et al*[5]. determined the crystal structure of *N*-benzoyl glycine and the title compound, $C_6H_5CONHCH_2COOH$, is non-centrosymmetric, space group $P2_12_12_1$, with the cell dimension, (23°), *a*=9.117Å, *b*=10.578 Å, *c*=8.870Å and *V*=855.4Å^3.

3.1 Molecular geometry

The optimized geometrical parameters, namely, bond lengths and angles calculated by HF, DFT/B3LYP with 6-31G(d,p) and 6-311++G(d,p) basis sets are listed in Table 1. Experimental data on the geometric structure obtained by Ringertz[10] are also listed in Table 1. From Table 1, it is noted that the bond lengths calculated by 6-311++G(d,p) basis set are always smaller than those calculated by 6-31G(d,p) for B3LYP method because diffuse function is considered in 6-311++G(d,p) basis set. In addition, the bond lengths calculated by HF method are always shorter than those calculated by B3LYP method because the electron correlations are neglected for HF method. Compared the calculated bond lengths and angles with the experimental data[10], it is noted that bond lengths and angles calculated by B3LYP/6-311++G(d,p) method are closer to the experimental data.

The hexagonal symmetry of the benzene ring is obvious from the bond lengths of the C_3-C_4 and C_2-C_3 bonds. The symmetry of the benzene ring is also evident from the C-C-C bond angles. The magnitudes of the C_3-C_4 and C_2-C_3 bonds are found to be 1.399Å and 1.400 Å, respectively, which is slightly bigger than double C=C bond length but shorter than the single C-C bond length (1.54 Å). The C-C-C bond angles of the benzene ring are all about 120.0°.

The C_{12}=O_{13} and C_{19}=O_{20} bond lengths are found to have magnitude of 1.225 Å and 1.207 Å at B3LYP/6-311++G(d,p) level, respectively, which are between double (C=O, 1.20Å) and single (C-O, 1.43Å) bond length and indicates its involvement in conjugation.

Interesting, the magnitudes of bond angles C_5-C_4-H_9 and C_3-C_4-H_9 are 121.2° and 118.4° at B3LYP/6-311++G(d,p) level, respectively, which indicates that the C_4-H_9 bond is not symmetrically disposed on C_4, rather it is tilted towards the C_{12}=O_{13} group due to

Table 1 — Optimized geometrical parameters of the title compound, bond lengths (Å) and bond angles (°)

Parameter	RHF		B3LYP		Experimental	parameter	RHF		B3LYP		Experimental
	6-31G(d,p)	6-311++G(d,p)	6-31G(d,p)	6-311++G(d,p)	Data		6-31G(d,p)	6-311++G(d,p)	6-31G(d,p)	6-311++G(d,p)	Data
C1-C2	1.385	1.385	1.395	1.393	1.396	C4–C3–C12	117.4	117.5	117.2	117.4	116.6
C2-C3	1.390	1.390	1.402	1.400	1.405	C3–C4-C5	120.3	120.3	120.4	120.4	119.7
C3-C4	1.390	1.390	1.401	1.400	1.407	C4–C5–C6	120.0	120.0	120.1	120.1	120.1
C4-C5	1.383	1.383	1.392	1.391	1.394	C1–C6–C5	120.0	120.0	119.9	119.8	120.1
C5-C6	1.386	1.386	1.397	1.395	1.400	C3–C12-O13	121.8	121.7	122.2	122.1	120.6
C6-C1	1.385	1.385	1.396	1.394	1.391	C3–C12-N14	116.8	116.8	116.5	116.6	117.9
C3-C12	1.500	1.502	1.502	1.501	1.496	O13–C12-N14	121.5	121.6	121.3	121.3	121.5
C12-O13	1.203	1.199	1.229	1.225	1.238	C12-N14-C16	120.2	120.4	120.0	120.6	121.2
C12-N14	1.353	1.353	1.368	1.366	1.336	N14-C16-C19	109.4	109.7	109.3	109.7	112.5
N14-C16	1.435	1.437	1.443	1.444	1.454	C16-C19-O20	125.0	125.1	124.9	125.2	127.0
C16-C19	1.505	1.505	1.512	1.510	1.513	C16-C19-O21	111.7	111.5	111.6	111.4	108.9
C19-O20	1.189	1.184	1.213	1.207	1.196	C1-C2-C3-C12	179.6	179.4	179.9	179.4	-
C19-O21	1.322	1.322	1.347	1.347	1.325	C2-C3-C12-N14	22.7	23.3	18.2	20.3	-
C2–C1–C6	120.0	120.0	120.1	120.1	120.1	C3-C12-N14-C16	-1.9	178.4	175.7	178.6	-
C1–C2–C3	120.2	120.3	120.3	120.3	119.5	C12-N14-C16-C19	-175.2	–176.3	–162.9	–173.1	-
C2–C3–C4	119.5	119.4	119.3	119.2	120.6	N14-C16-C19-O21	-176.7	–177.1	–178.0	–178.1	-
C2–C3–C12	123.1	123.1	123.5	123.4	123.3	N14-C16-C19-O20	3.8	3.4	2.0	2.0	-

propensity of oxygen atom to form H-bonding with the H atom of the C_4-H_9 bond. It is noted that the H_9-O_{13} bond length is 2.497Å, while the C_4-O_{13} bond length is 2.829 Å. In addition, the magnitudes of bond angles C_{12}-N_{14}-H_{15} and C_{16}-N_{14}-H_{15} are 121.8° and 116.6° at B3LYP/6-311++G(d,p) level, respectively, while the H_{15}-O_{20} bond length is 2.279Å, which indicates the presence of H-bonding between H_{15} and O_{20} atoms. The hydrogen bond lengths and angles of NBG are listed in Table 2.

3.2 Vibrational assignments

In order to obtain the spectroscopic signature of NBG, we performed a frequency calculation analysis. Table 3 presents the calculated vibrational frequencies, IR intensities, Raman activity and normal mode descriptions (characterized by PED) of NBG at B3LYP/6-311++G(d,p) method. Jayarama *et al*[5]. recorded the FTIR and FT-Raman spectrum in the range 400-4000 cm^{-1}, so we also listed the experimental vibrational frequencies in Table 3. It is customary to scale down the calculated harmonic frequencies in order to improve the agreement with the experiment. Vibrational frequencies calculated at B3LYP/6-311++G(d,p) level were scaled[11] by 0.958 in the 1700-4000 cm^{-1} region and 0.983 for B3LYP/6-311++G** in the 400-1700 cm^{-1}. Any discrepancy noted between the observed and the calculated frequencies may be due to the two facts: one is that the experimental results belong to solid phase and theoretical calculations belong to gaseous phase; the other is that the calculations have been actually done on a single molecule contrary to the experimental values recorded in the presence of intermolecular interactions. The descriptions concerning the assignment have also been presented in Table 3.

Figure 2 shows the correlation between calculated and experimental vibrational frequencies of NBG. It is noted that the calculated frequencies by B3LYP method are all in good agreement with the experimental frequencies. The observed and simulated IR and Raman spectra are shown in Figs 3 and 4, respectively. Here, the observed IR and Raman spectra come from Jayarama *et al*[5]. Calculated Raman

Table 2 — Selected hydrogen bond lengths (Å) and bond angles (°) calculated by B3LYP/6-311++G(d,p) method

D-H..A	*d*(D-H)	D(H…A)	D(D…A)	∠DHA
C_4-H_9…O_{13}	1.083	2.497	2.829	96.3
N_{14}-H_{15}…O_{20}	1.010	2.279	2.717	104.7
O_{21}-H_{22}…O_{20}	0.969	2.309	2.250	152.1

Table 3 — Calculated and experimental fundamental frequencies (cm^{-1}) for the title compound with B3LYP/6-311++G(d,p) method

Sr No.	Calculated frequencies	Experimental[a] (IR)	Assignments [PED]
1	397.13(0.93, 0.28)		Φ(ring)[68]
2	443.61(11.41, 0.87)	430.2	Φ(ring)[47], δ(N-H)[32]
3	469.64(69.23, 1.20)		δ(N-H)[71]
4	495.77(4.52, 2.40)		$\delta(C\text{-}H)_{CH2}$[38], δ(O-H)[32]
5	526.23(56.81, 0.23)	535.4	δ(CCO)[68]
6	603.86(30.99, 2.32)		$\delta(OCO)_{COOH}$ [70]
7	607.32(0.31, 5.74)		α(ring)[80]
8	623.40(107.10, 0.21)		$\delta(C\text{-}H)_{CH2}$ [37], δ(O-H)[52]
9	659.99(1.74, 4.04)		α(ring)[74]
10	674.29(10.67, 0.17)	652.2	δ(C-H)oop[88]
11	692.52(81.49, 0.29)	712.5	δ(C-H)oop[85]
12	783.41(4.54, 2.46)		δ(C-H)oop[52], δ(C-C)[34]
13	806.55(2.28, 2.06)		ν(C-C)[72],
14	824.82(0.79, 0.55)	850.6	δ(C-H)oop[95]
15	903.99(34.19, 22.08)	877	$\delta(C\text{-}H)_{CH2}$ [65]
16	907.95(2.01, 0.28)		δ(C-H)oop[95]
17	952.95(0.77, 0.01)		δ(C-H)oop[95]
18	970.26(0.33, 0.46)		δ(C-H)oop[90]
19	971.93(3.00, 0.62)		$\delta(C\text{-}H)_{CH2}$ [99]
20	976.28(1.31, 43.14)		α(ring)[99]
21	1005.56(1.99, 12.38)	1011.8	δ(C-H)ip[90]
22	1047.25(26.74, 3.11)		ν(C-N)[42], δ(C-H)ip[45]
23	1063.61(41.91, 0.29)	1094.9	δ(C-H)ip[85]
24	1119.73(264.92, 0.27)		ν(C-O)[90]
25	1136.51(0.95, 4.99)		δ(C-H)ip[95]
26	1140.35(86.42, 13.55)		ν(C-N)[42], ν(C-C)[35]
27	1158.70(0.07, 4.00)	1175.4	δ(C-H)ip[90]
28	1188.61(0.76, 6.54)		$\delta(C\text{-}H)_{CH2}$ [95]
29	1211.82(26.31, 65.86)		δ(N-H)[34], ν(C-C)[27], $\delta(C\text{-}H)_{CH2}$ [32]
30	1262.77(1.09, 11.60)		δ(O-H)[48], $\delta(C\text{-}H)_{CH2}$ [34]
31	1280.65(1.47, 0.98)		α(ring)[92]
32	1299.10(1.07, 0.79)		δ(C-H)ip[90]
33	1357.55(267.45, 7.30)	1334.9	ν(C-C)[34], $\delta(C\text{-}H)_{CH2}$[45]
34	1415.88(2.62, 2.35)	1405.6	ν(C=C)[65]
35	1426.63(22.43, 5.30)		$\delta(C\text{-}H)_{CH2}$ [88]
36	1456.05(118.56, 1.74)		δ(N-H)+α(ring)
37	1477.22(257.57, 16.10)	1486.5	δ(N-H)[72]
38	1554.23(13.76, 8.86)		ν(C=C)[83]
39	1575.67(8.65, 90.47)	1566.2	ν(C=C)[90]
40	1647.27(304.26, 47.12)	1613.2	$\nu(C{=}O)_{NCO}$[85]
41	1738.00(249.12, 11.58)	1749.9	$\nu(C{=}O)_{COOH}$ [87]
42	2913.41(25.61. 144.44)		$\nu(C\text{-}H)_{CH2}$[99]
43	2934.62(3.93, 66.48)	2978.9	$\nu(C\text{-}H)_{CH2}$[99]
44	3037.04(1.36, 32.64)		ν(C-H)ip[100]
45	3043.93(4.10, 106.80)		ν(C-H)ip[100]
46	3053.02(19.66, 58.28)		ν(C-H)ip[100]
47	3062.66(12.52, 209.43)		ν(C-H)ip[100]
48	3073.58(5.01, 139.52)	3081.7	ν(C-H)ip[100]
49	3468.43(61.06, 61.47)	3343.6	ν(N-H) [100]
50	3609.56(94.60, 163.33)		ν(O-H)[100]

α: planar ring deformation, Φ: non-planar ring deformation, ν: stretching, δ: bending, ip: in-plane deformation, oop: out-of-plane deformation. [a] Data from (Ref. 5)

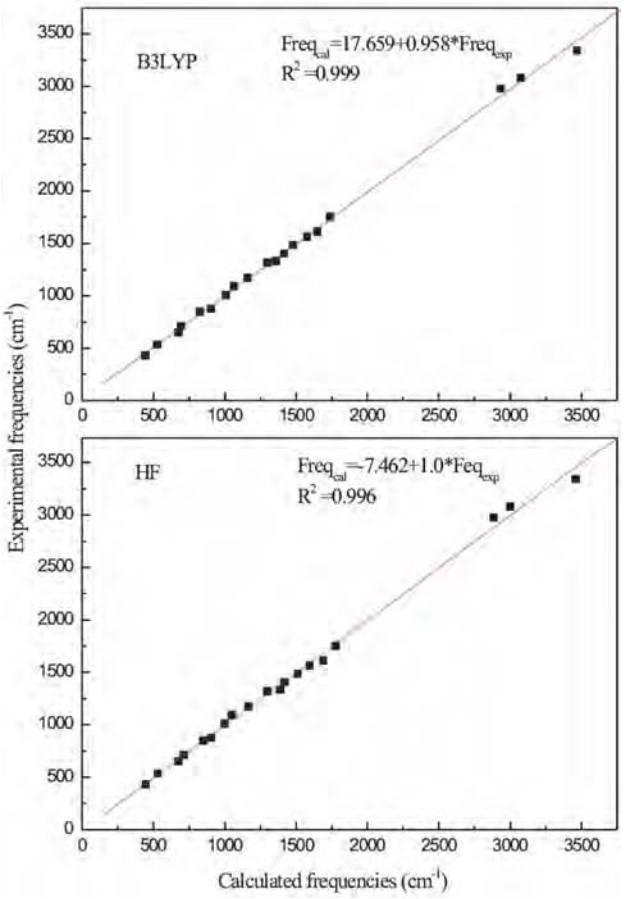

Fig. 2 — Correlation graphics of calculated and experimental frequencies of the title compound by B3LYP and HF methods

activities and IR intensities help us to distinguish and more precisely assign those fundamentals which are close in frequency.

3.2.1 C-H vibrations

According to Roeges[12], the CH stretching vibrations of the phenyl ring are expected in the region 3120-3000 cm^{-1}. In this region, the bands are not affected appreciably by the nature of the substituent. In the present theoretical study, the calculated values of these modes for NBG are 3037.04, 3043.93, 3053.02, 3062.66, 3073.58 cm^{-1} at B3LYP level. Experimentally the band at 3081.7 cm^{-1} is observed in the IR spectrum for NBG. The C-H out-of-plane deformation is usually observed between 1000 and 700 cm^{-1} (Ref 12). These δ(C-H) out-of-plane modes are observed at 652.2, 712.5, 850.6 cm^{-1} for NBG in the IR spectrum. The DFT calculation gives these modes at 674.29, 692.52, 783.41, 824.82, 907.95, 952.95, 970.26 cm^{-1}. The δ(C-H) in-plane deformation vibrations are observed at 1011.8, 1094.9

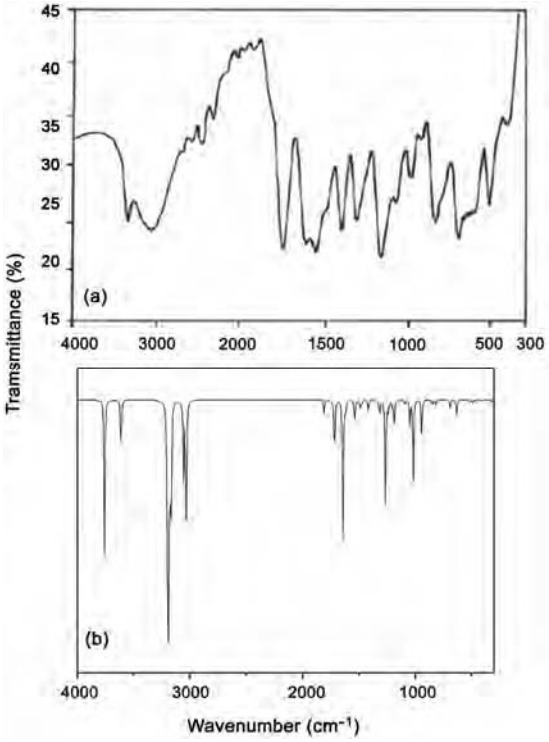

Fig. 3 — (a) Observed IR spectrum, (b) Theoretically IR spectrum of N-benzoyl glycine by B3LYP/6-311++G(d,p) method

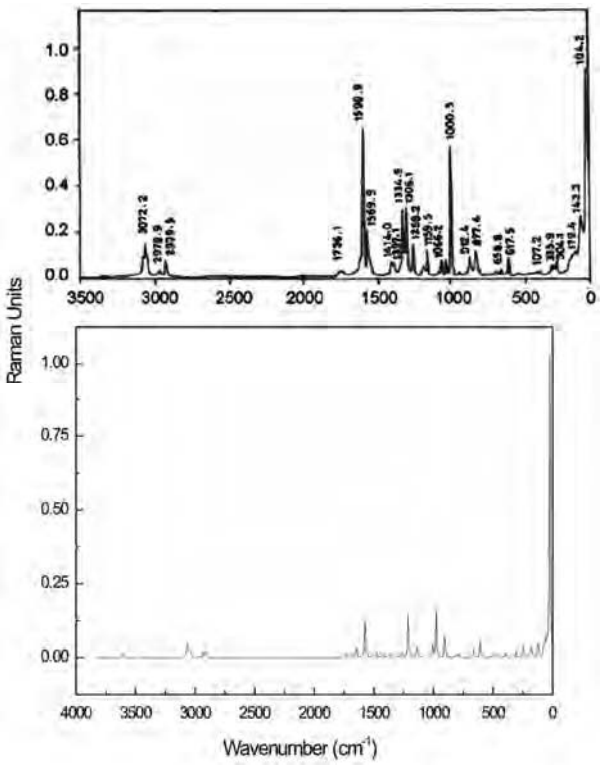

Fig.4 — (a) Observed Raman spectrum, (b) Theoretically Raman spectrum of N-benzoyl glycine by B3LYP/6-311++G(d,p) method

and 1175.4 cm^{-1}, and the DFT calculation gives these modes at 1005.56, 1047.25, 1063.61, 1136.51, 1158.70, 1299.10 cm^{-1}.

3.2.2 C=O vibration

Since the C=O group is a terminal group, only the carbon is involved in a second chemical bond. This reduces the number of force constants determining the spectral position of the vibration. Almost all carbonyl compounds have a very intense and narrow peak in the range 1800-1600 cm^{-1}. This is why this region is considered as a very important region by organic chemists. If a compound contains a carbonyl group the absorption caused by C=O stretching is generally the strongest present. For example, El. Shahawy *et al*[13]. reported a value of 1640 cm^{-1} in the IR spectrum as $\upsilon_{C=O}$ for paracetamol and at 1965 cm^{-1} for 5-amino-2-nitro-benzoic acid.

In this present study, the C=O stretching vibration[5] is observed at 1613.2, 1749.9 cm^{-1}, while DFT calculation gives C=O stretching mode at 1647.27, 1738.00 cm^{-1}. This shows that the observed C-O vibration is in excellent agreement with theoretically predicted frequency obtained by B3LYP/6-311++G(d,p) method. Any deviation of the calculated wavenumber for this mode can be attributed to the under estimation of large degree of π-electron delocalization due to conjugation or formation of hydrogen bonds.

3.2.3 N-H stretching vibration

Hetero aromatics containing an N–H group show its stretching absorption in the region 3500-3220 cm^{-1}. The position of absorption in this region depends upon the degree of hydrogen bonding, and hence upon the physical state of the sample or the polarity of the solvent[14]. For NBG, the N-H stretching mode is observed at 3343.6 cm^{-1}. DFT calculation gives the N-H stretching vibration at 3468.43 cm^{-1}. The N-H stretching wavenumber is red shifted by 125 cm^{-1} in the IR with a strong intensity from the computed wavenumber, which indicates the weakening of the N_{14}-H_{15} bond resulting in proton transfer to the neighbouring oxygen.

3.2.4 C-N vibrations

The medium to weak absorption bands for the C-N linkages in amines appear in the region 1200-1020 cm^{-1}. It is a difficult task to identify the C-N stretching in the side chain from other vibrations. Jeyavijayan *et al*[15]. have observed the C–N stretching vibration between 1578-1366 1375 cm^{-1} in hypoxanthine. For NBG, C-N stretching vibrations are not observed, while DFT calculation gives the C-N stretching vibration at 1047.25 cm^{-1}.

3.2.5 Deformation vibrations

Six ring deformation frequencies are observed in benzene. Of these, three arise from in-plane bending vibrations, corresponding to 606 and 1010 cm^{-1} mode and the remaining three are derived from out-of-plane bending vibrations corresponding to 404 and 711 cm^{-1} mode of vibrations. The vibrational modes of the benzene ring in plane deformation are not reported by Jayarama *et al*[5]., DFT calculation gives the α(ring) vibrational mode at 607.32, 659.99, 976.28, 1280.65, 1456.05 cm^{-1} and gives the vibrational mode of benzene ring out of plane deformation (Φ(a ring)) at 397.13, 443.61 cm^{-1}.

3.2.6 NBO analysis

The NBO analysis is an effective tool to interpret the hyper conjugative interaction and electron density transfer from the filled lone pair electron. DFT/B3LYP level has been used to investigate the various second-order interaction between the filled orbitals of one sub-system and vacant orbitals of another sub-system and predicted the delocalization or hyperconjugation[16]. The hyperconjugative interaction energy was deduced from the second-order perturbation approach:

$$E(2) = -n_\sigma \frac{\langle \sigma | F | \sigma \rangle^2}{\varepsilon_{\sigma^*} - \varepsilon_\sigma} = -n_\sigma \frac{F_{ij}^2}{\Delta E}$$

where $\langle \sigma | F | \sigma \rangle^2$, or F_{ij}^2 is the Fock matrix element between i and j NBO orbitals, $\varepsilon_{\sigma*}$ and ε_σ are the energies of σ* and σ NBO's and n_σ is the population of the donor σ orbital.

The larger $E^{(2)}$ value, the more intensive is the interaction between electron donors and acceptor. That is to say the more donation tendency from electron donors to electron acceptors, the greater the extent of conjugation of the whole system[17].

The intra-molecular interaction is formed by the orbital overlap between σ(C_{19}-O_{20}) and σ*(C_{19}-O_{20}), which results intra-molecular charge transfer causing stabilization of the system. The most important interactions in the title compound having lone pair O_{13} with anti-bonding C_{12}-N_{14} and C_3-C_{12}, results the stabilization of 24.43 and 18.39 kJ/mol, respectively.

Table 4 — Second-order perturbation theory analysis of Fock matrix in NBO basis corresponding to the intramolecular of the title compound

Donor NBO(i)	Acceptor NBO(j)	$E^{(2)a}$ (kJ/mol)	E(j)-E(i)[b] a.u.	F(i,j)[c] a.u.
$\sigma(C_{19}\text{-}O_{20})$	$\sigma^*(C_{19}\text{-}O_{20})$	0.79	0.40	0.017
$\sigma(N_{14}\text{-}C_{16})$	$\sigma^*(C_3\text{-}O_{12})$	2.37	1.19	0.048
$\sigma^*(N_{14}\text{-}C_{16})$	$\sigma^*(C_{19}\text{-}O_{21})$	2.04	1.09	0.043
$LP2O_{13}$	$\sigma^*(C_{12}\text{-}N_{14})$	24.43	0.71	0.120
$LP2O_{13}$	$\sigma^*(C_3\text{-}O_{12})$	18.39	0.67	0.101
$LP2O_{20}$	$\sigma^*(C_{19}\text{-}O_{21})$	32.42	0.63	0.129
$LP2O_{20}$	$\sigma^*(C_{16}\text{-}O_{19})$	18.07	0.65	0.099
$LP1N_{14}$	$\sigma^*(C_{12}\text{-}O_{13})$	54.05	0.30	0.114
$LP2O_{21}$	$\sigma^*(C_{19}\text{-}O_{21})$	45.86	0.35	0.114
$LP2O_{20}$	$\sigma^*(N_{14}\text{-}H_{15})$	0.84	0.70	0.022
$LP2O_{13}$	$\sigma^*(C_4\text{-}H_9)$	0.67	0.60	0.018

[a]$E^{(2)}$ means energy of hyperconjugative interaction; [b]Energy difference between donor and acceptor i and j NBO orbital; [c]F(i,j) is the Fock matrix element between i and j NBO orbitals

Table 5 — Atomic charges for optimized geometry of the title compound with 6-311++G(d,p) basis set

Atom no.	RHF	B3LYP	Atom no.	HF	B3LYP	Atom no.	RHF	B3LYP
C_1	–0.29	–0.27	H_7	0.21	0.17	O_{13}	–0.43	–0.33
C_2	–0.29	–0.23	H_8	0.21	0.16	N_{14}	–0.22	–0.08
C_3	1.21	1.15	H_9	0.25	0.21	H_{15}	0.29	0.25
C_4	–0.08	–0.21	H_{10}	0.21	0.17	C_{16}	–0.31	–0.31
C_5	–0.42	–0.37	H_{11}	0.20	0.16	C_{19}	0.38	0.21
C_6	–0.29	–0.19	C_{12}	–0.79	–0.81	O_{20}	–0.40	–0.31
						O_{21}	–0.24	–0.15

The interactions between lone pair O_{20} with anti-bonding C_{19}-O_{21} and C_{16}-C_{19} result into the stabilization of 32.42 and 18.04 kJ/mol, respectively, which denote larger delocalization. The interaction between the lone-pair $LP2O_{20}$ and the anti-bonding orbital $\sigma^*(N_{14}\text{-}N_{15})$ is 0.84 kJ/mol. The interaction between the lone-pair $LP2O_{13}$ and the anti-bonding orbital $\sigma^*(C_4\text{-}O_9)$ is 0.67 kJ/mol. The $E^{(2)}$ value is chemically significant and can be used as a measure of the intramolecular delocalization and these results are presented in Table 4.

3.3 Mulliken charges

The atomic charge in molecules is fundamental to chemistry. For instance, atomic charge has been used to describe the processes of electronegativity equalization and charge transfer in chemical reactions, and to model the electrostatic potential outside molecular surfaces[18].

Mulliken atomic charges calculated at the B3LYP/6-311++G(d,p) and RHF/6-311++G(d,p) methods are presented in Table 5. It is noted from Table 5 that the charge distribution is related with the computational method. For example, the charge of N_{14} atom is −0.22 for RHF level and-0.08 for B3LYP level.

It is noted that the five hydrogen atomic charges of benzene ring calculated by B3LYP method are always smaller than those calculated by RHF method. Their values are found to be 0.17, 0.16, 0.21, 0.17, 0.16 at B3LYP/6-311++G(d,p) level for H_7, H_8, H_9, H_{10}, H_{11}, respectively. Obviously, the charge on H_9 atom is bigger than those on other hydrogen atoms. Similar trend is being observed for the charge on H_{15} atom and the charge on H_{15} atom is 0.25. The charges on O_{13} and O_{20} atoms increase from RHF to DFT method and are −0.33 and −0.31 at DFT level of calculation, respectively. The charge on O_{21} atom is −0.15 at DFT level of calculation, which is bigger than the charges on O_{13} and O_{20} atoms. From above analysis, we can conclude that the presence of the higher charge on H_9 atom and the lower charge on O_{13} atom may suggest the formation of intramolecular interaction in solid forms. The similar conclusion can be obtained for the intramolecular interaction between O_{20} and H_{15}.

Table 6 — HOMO-LUMO energy calculated by B3LYP/6-311++G(d,p) method

Method	B3LYP/6-311++G**
Parameters	
HOMO	–0.26394 a.u.
LUMO	–0.05247 a.u.
Energy gap (ΔE)	0.21147 a.u.

3.4 HOMO-LUMO analysis

The highest occupied molecular orbital (HOMO) and lowest unoccupied molecular orbital (LUMO) are the main orbital take part in chemical stability[19]. The HOMO represents the ability to donate an electron, LUMO as an electron acceptor represents the ability to obtain an electron. The electron transition absorption corresponds to the transition from the ground to the first excited state and is mainly described by an electron excitation from the HOMO to the LUMO. HOMO and LUMO energies calculated by B3LYP/6-311++G(d,p) method, are listed in Table 6. The calculated self-consistent field (SCF) energy of the title compound is-628.851a.u.

4 Conclusions

We have carried out DFT and *ab-initio* calculations on the structure and vibrational spectrum of the title compound. Comparison between the calculated and

experimental structural parameters indicates that B3LYP results are in good agreement with experimental ones. The analysis of the bond length and angle for the title compound shows that there exist the H-bonding between H_9 and O_{13} and H_{15} and O_{20} atoms. Vibrational frequencies calculated by B3LYP/6-311++G(d,p) method agree very well with experimental results. On the basis of agreement between the calculated and observed results, assignments of the fundamental vibrational modes of the title compound were assigned based on the results of the PED output obtained from normal coordinate analysis. NBO analysis substantiates the weak C-H…O and N-H…O hydrogen bond, which is consistent with the analysis of molecular structure.

Acknowledgement

We gratefully thank the National Natural Science Foundation of China (Grant 10774039) and the grant from Development Program in Science and Technology of Henan Province (No. 102300410114 and No. 112300410206), Henan University of Science and Technology for Young Scholars (No.2009QN0032) for their support of this work.

References

1 Kaino T, Cai B & Takayama K, *Adv Funct Mater,* 12 (2002) 599.

2 Geis W, Sinta R, Mowers W, Deneault S J, Marchant M F, Krohn K E, Spector S J, Calawa D R & Lyszczarz TM, *Appl Phys Lett,* 84 (2004) 3729.

3 Schneider A, Neis M, Stillhart M Ruiz, B, Khan R U A & Gunter P, *J Opt Soc Am B,* 23 (2006) 1822.

4 Nicould J F & Twieg R J, in: Chemla D S, Zyss J (Eds), *Nonlinear Optical Properties of Organic Molecules and Crystals,* Academic Press, London, 1987

5 Jayarama A, Ravindra H J & Dharmaprakash S M, *Materials Chem and Phys*, 113 (2009) 91.

6 Frisch M J, Trucks G W, Schlegel H B, Scuseria G E, *et al*. *J A GAUSSIAN* 03, Revision B02, Gaussian Inc: Pittsburgh PA, 2003.

7 Becke A D, *J Chem Phys,* 98 (1993) 5648.

8 Sundius T, *MOLVIB: A program for harmonic force field calculations, QCPE program* No 807, 2002.

9 Keresztury G, Holly S, Varga J, Besenyei G, Wang AY & Durig J R, *Spectrochim Acta A,* 49 (1993) 2007.

10 Ringertz By Hans, *Acta Cryst B*, 27（1971）285.

11 Sundaraganesan N, Ilakiamani S, Saleem H, Wojciechowski P M & Michalska D, *Spectrochim Acta, A,* 61 (2005) 2995.

12 Roeges N P G, *A Guide to Complete Interpretation of Infrared Spectra of Organic Structures*, Wiley, New York, 1994.

13 El-Shahawy A S, Ahmed S M & Sayed N K, *Spectrochim Acta A,* 66 (2007) 143.

14 Gunasekaran S, Varadhan S R & Manoharan K, *Asian J Phys,* 2(3) (1993) 165.

15 Jeyavijayan S & Arivazhagan M, *Indian J Pure & Appl Phys*, 48 (2010) 869.

16 Thomson H W & Torkington P, *J Chem Soc,* (1945) 640.

17 Sebastian S & Sundaraganesan N, *Spectrochim Acta A*, 75 (2010) 941.

18 Cieplak P, *J Comp Chem,* 12 (1991) 1232.

19 Gunasekaran S, Balaji R A, Kumerasan S, Anand G & Srinivasan S, *Can J Anal Sci Spectrosc*, 53 (2008) 149.